A Study on Nanofiber-Reinforced Thermoplastic Composites (II): Investigation of the Mixing Rheology and Conduction Properties

K. LOZANO,[1] J. BONILLA-RIOS,[2] E. V. BARRERA[3]

[1] Department of Engineering, The University of Texas Pan American, Edinburg, TX 78539

[2] Instituto Tecnologico y de Estudios Superiores de Monterrey, Monterrey, N. L., Mexico

[3] Department of Mechanical Engineering and Materials Science, Rice University, Houston, TX 77005

Received 10 June 2000; accepted 4 July 2000

ABSTRACT: This article is portion of a comprehensive study on the development of nanofiber-reinforced polymer composites for electrostatic discharge materials and structural composites. Vapor-grown carbon fibers with an average diameter of 100 nm were used as a precursor and model fiber system for carbon nanotubes. These nanofibers were purified and functionalized to provide for an open network of high-purity nanofibers. Banbury-type mixing was used to disperse the nanofibers in the polymer matrix. Rheological and microscopic analysis showed that the high shear processing of the polymer/nanofiber mixture led to a homogeneous dispersion of nanofibers with no agglomerates present and no shortening of the nanofibers. The shear thinning behavior of polymeric materials helps in the mixing of the nanofibers to form the composites. A percolation threshold for electrical conduction of 9–18 wt % was observed for the highly dispersed nanofiber networks. The electrical behavior of these materials was not affected by changes in humidity. Microscopic analysis showed highly dispersed nanofibers with no indications of porosity. These conducting polymers are well suited for electrostatic discharge applications, and might well become multifunctional materials for strength/electrical applications. © 2001 John Wiley & Sons, Inc. J Appl Polym Sci 80: 1162–1172, 2001

Key words: composite; rheological analyses; nanofiber; nanotubes; static dissipative

INTRODUCTION

In this study, the mixing of nanofibers in thermoplastics, namely vapor-grown carbon fibers (VGCFs) in polypropylene (PP), was directed toward achieving a high degree of dispersed nanofibers and not a segregated network. Conducting polymers as multifunctional materials are sought. Nanofibers of VGCFs were purified, functionalized, and mixed with PP to produce dispersions on a per nanofiber scale. This morphology lends itself more toward development of multifunctional materials that can enhance mechanical as well as electrical and thermal properties.

The rapid development of electronic devices and as a consequence the rise of electrostatic discharge (ESD), electromagnetic interference (EMI), and radio frequency interference (RFI) have

Correspondence to: K. Lozano.

Contract grant sponsor: National Science Foundation; contract grant number: DMR-9357505.

Contract grant sponsor: Texas Higher Education Board; contract grant number: 003604-056.

Contract grant sponsor: National Aeronautics and Space Administration; contract grant number: NCC 9-77.

Contract grant sponsor: Consejo Nacional de Ciencia y Tecnologia (CONACYT).

Journal of Applied Polymer Science, Vol. 80, 1162–1172 (2001)

prompted the development of new conductive materials to prevent devastating effects on the quality and reliability of manufactured electronics.[1–9] ESD accounts for 40% of the failures that occur in the electronics industry at an estimated cost of billions of dollars, annually.[10,11] To overcome such costs, several different combinations of filled plastics with carbon fibers, metal flakes and fibers, metal-coated fibers, and carbon black as well as blends of copolymers and chemically modified polymers have been investigated.[4,12–22] In this work, the use of nanofibers for development of conducting polymers and structural materials will be studied where a different dispersion is sought from the segregated networks often seen for carbon black[4] and other dispersed conductive media.[1] Recently, Sandler et al.[23] showed that low concentrations of nanofibers could be used to obtain ESD polymers, yet they relied on a loose network that did not have the potential of enhancing the strength of the composites. Herein, highly dispersed nanofiber dispersion is sought to further investigate the potential for developing structural composites as well.

In this article, the process rheology of mixing nanofiber reinforced composites with several nanofiber loadings is coupled to the study of the electrical properties that result in the composites produced. The VGCFs used in this study were used in as-received, purified, pelletized, and functionalized conditions where the purification and functionalization schemes were worked out in this research through process optimization. Nanofiber mixing in polypropylene was achieved by the conventional Banbury method where high shear zones lead to nanofiber deagglomeration and high dispersion. Torque rheological and other flow measurements showed that an ease of processing was achieved (for 14–20-g quantities of material) with increasing shear rates where the effect of nanofiber concentration became almost negligible. Microscopic analyses showed that a high degree of dispersion was achieved. Standard ESD measurements showed that a network of dispersed nanofibers lead to a percolation threshold at 9–18 wt % of VGCFs in PP. The VGCF concentration range was studied up to 60 wt %. A similar percolation threshold is seen for VGCFs in polyethylene (PE), and a significant drop in resistivity is seen for a single wall nanotube (unpurified)/epoxy system where all these composites are suited for operation in a range of humidity conditions.

Therefore, the objectives of this article were to better understand the utility of nanofibers for multifunctional materials (structural/electrical), where VGCFs are used as a precursor system to working with nanotubes. The ability to mix the nanofibers in polymers is sought via a rheological study, and the role of nanofibers in property enhancement is of interest, and will be correlated to the role of nanotubes in composites.

BACKGROUND

Development of nanofiber, particularly nanotube-reinforced composites, has been limited by difficulties associated with availability of nanotubes and observed high viscosity processing. Single-wall nanotubes (SWNTs) and multiwall nanotubes (MWNT's) have a hollow core, and are of similar lengths to the VGCFs used in this study. Differences occur in the defect levels present and the size of the diameters.[24–26] Because SWNTs and MWNTs are by far less abundant at this time, VGCFs are ideal for studying the basic role of nanofibers in polymer systems. In fact, the various steps likely to be used to produce nanotube composites are the steps used to produce nanocomposites using nanofibers with an average diameter of 100 nm. Although there is a significant difference from single-wall nanotubes (diameters on the order of 1 nm), the size of VGCFs is within one order of magnitude of MWNTs and SWNT ropes. In review of the recent research using SWNTs, where only ropes are used,[27–29] it is evident that the processing in this research will clearly be productive at producing high dispersions of nanotubes for multifunctional polymeric material applications.

Recent work of mixing polymers with carbon black, nanosize clays, submicron whiskers, or particles is related to the mixing of nanofibers in polymers.[30–35] The research and development of rigid-rod polymers and the field of liquid crystal polymers is also applicable. Recently, Tjong and Meng[36] studied the processing of potassium titanate whiskers (0.5–1 μm in diameter) in a polycarbonate. Although the size of these reinforcements is not nanoscale, they identified important rheological aspects that need to be addressed to understand the dispersion of nanofibers in polymers. They noted that the polymer is altered by the reinforcement due to surface interactions associated with whisker preparation. An increase in whisker concentration lead to an increase in mod-

uli, a decrease in tensile strength, a decrease in torque (measured in a torque rheometer), and an increase in polymer degradation. They also observed that it was easier to align the whiskers as the viscosity decreased. Nanofibers and nanotubes have surface areas up to two orders of magnitude higher that the potassium titanate whiskers and Lozano et al.[37] showed that for VGCFs the interfaces created might place a significant role. Furthermore, because there is significantly more interface, there is also less space between nanofibers, leaving little space for the polymer to actively alter during deformation processes.

The use of carbon black for dissipative materials involves setting up a segregated network of the carbon black and polymer. Although a different network was sought in this work, the rheological nature of mixing carbon black in polymers is of interest. The idea of "bound rubber" or the influence carbon black can have on interactions with polymer additives is important to what might be observed with nanofiber systems. They, like many polymer additives, influence viscosity and other rheological properties independent of particle scaling. Bound rubber is a factor for determining the interaction conditions of carbon black with polymer additives in rubber. A factor such as this might well be useful for the evaluation of interactions of nanofibers with various advanced polymers. The various studies of rigid-rod polymers that led to the development of poly(paraphenylene benzobisoxazole) (PBO) showed that molecular polymeric composites are similar in a number of ways to the nanofiber composites being developed today.

Nanofibers are already seeing use in conducting paints applications, in the case of automotive side mirror housings, and their use for other applications is expected to increase.[38,39] ESD materials are needed for electronic packaging purposes, for garments, dissipative chairs, work benches and floor mats for the personnel working in the electronic manufacturing site, to name a few applications. Table I lists some materials that fall into the static dissipative range necessary to provide ESD protection. Their values are low enough to dissipate static energy, but not too low to produce sparking.

Evaluation of the ESD of polymer composites can be accomplished by volumetric and surface resistivity measurements (VR or SR, respectively). Volume resistivity was obtained by measuring sample resistance and then converting it to resistivity while taking geometric considerations into account. The surface resistivity is defined as the ratio of the DC voltage to the current flowing between two electrodes of specific configuration. Measuring resistivities presents some level of concern, in the case where two-point probe or four-point probe methods are used. Care is taken to follow standard resistivity testing procedures such as those from the American standard for testing and materials (ASTM) and the American national standards institute (ANSI). Samples were also evaluated in two different laboratories and under differing humidity conditions. Four-point probe and dielectric breakdown tests were conducted to evaluate the sheet materials produced. In some cases, the discharge times (DT) were obtained for the volumetric resistivity studies. All tests were evaluated in such a way as to determine whether the materials were isotropic.

Table I Comparison of ESD Polymeric Materials

ESD Material	Surface Resist Range (Ω/square)
ESD nylons[18]	10^6–10^{12}
Thermoplastic resin/chopped linear carbonaceous fibers[11]	10^4–10^{10}
PC 85%/PAN 10%/Gr fiber 5%[4]	10^3–10^4
Nylon 85%/6/6/15% fiberglass[4]	10^3
Carbon black filled PP, PE, PC[4]	10^7
Carbon black/nylon 6/6[4]	10^7
Carbon black/PP/20% fiber glass[4]	10^5

The previous article discussed the thermophysical aspects of these materials,[40] and this article will focus on the electrical properties while relating process rheology to the final material performance. An ongoing research is looking for methods of lowering the percolation threshold for highly dispersed nanofiber conducting polymers and the influence of nanofiber surface preparation on mixing conditions. Two other article will deal more directly with achieving mechanical strength enhancements and or highly aligned nanofiber conditions.

EXPERIMENTAL

Materials Purification and Functionalization

Carbon nanofibers called Pyrograf-III™ were obtained from Applied Sciences, Inc. Pyrograf is produced by a catalytic process of hydrocarbons in

the vapor state. These VGCFs have circular cross sections (with diameters varying from 20 to 200 nm) and central hollow cores usually called filaments, with diameters of a few tenths of nanometers. Kilogram quantities are available enabling composites development to a higher scale than that seen in current MWNT and SWNT composite research.[25,41–43] VGCFs in as-received, needing purification, and pelletized, having a latex surface treatment and compacted to reduce dust, were obtained for this research. VGCFs were observed by scanning electron microscopy to be highly tangled agglomerates having dispersed amorphous carbon and metal catalysts.

To utilize the VGCFs, both purification and functionalization processes were needed to remove the unwanted products, providing opening of the highly tangled nests of nanofibers without shortening the fibers. Friend et al.[44] reported purification methods for Hyperion nanofibers, which led to shortening the nanofibers. Instead, in this research, purification was conducted by refluxing in dichloromethane for 5 days at a temperature of 35°C, followed by several deionized water washings and refluxing for 24 h at 90°C.[45] The nanofibers were rinsed again, vacuum filtered (Whatmat filter cat# 1440090 #40 Ashless) for 24 h and dried in air at 120°C for 48 h. Following purification, functionalization required to activate functional groups along the nanofibers was conducted. Different approaches were evaluated including: oxidation in air at 550°C, refluxing in HNO_3 (65% solution or concentrated), H_2SO_4 (65% solution), and mixtures of these acids. A Nicolet Magna Fourier transform infrared (FTIR) spectrometer was used to evaluate the purification and functionalization processes. For FTIR attenuated total reflectance (ATR) measurements, an ATR attachment with a Ge internal reflectance element with an endface angle of 45° was used. Composite production was conducted using as-received, pelletized, purified, and all the various functionalized conditions.

PP is a very well-known thermoplastic that is commercially available in different grades with different types of additives leading to a range of bonding conditions and possibilities for reactivity. PP is basically a nonpolar semicrystalline polymer with low surface tension. Pelletized, additive free PP HLM-020 from Phillips 66, was selected as the composite matrix. It was selected as a natural homopolymer so that PP/nanofiber interactions could be isolated from additives or copolymers effects. Other polymers used to help establish the baseline processing conditions included: Acetal, ABS, ASA, PE, PEEK, PE, and PET and were used in their commercial forms.

Nanofiber Reinforced Composite Preparation

The composites were prepared by mixing the VGCFs with the PP matrix in a Haake miniaturized internal mixer Rheomix 600 (MIM). The mixing process consisted of distributive mixing where the nanofibers where spread over different positions within the chamber and dispersive mixing where the application of high shear rates was required to overcome the nanofiber agglomerates. Different compositions by weight percent were prepared ranging from 0 to 60% wt of nanofibers. After mixing, the material was compression molded at a temperature of 170–200°C to form thin sheets.[40] Each sample weighed between 14 and 20 g.

Microscopic Analyses

The quality of the mixing is an important parameter to quantify, therefore microscopic analyses were conducted with an optical transmittance microscope and a reflectance optical microscope to identify the level of dispersion for different processing conditions. Given the microscopic observations, adjustments on the time of mixing, temperature, and the speed of the rotors were performed. The samples were analyzed using the NIH imagescan program that analyzes the images numerically using 256-grayscale values. Histograms and standard deviation values were obtained for different levels of VGCF concentration with different processing conditions. The morphology of the composites was analyzed by a combination of scanning and transmission electron microscopy techniques (SEM and TEM, respectively). SEM samples were gold sputtered to prevent charging although high concentration samples did not require this because they were conductive. The TEM samples were taken from specimen surfaces microtomed at room temperature.

Rheological Analysis

Processing data of the composites during mixing were recorded from the HAAKE torque rheometer where information of torque, temperature, and rpm was obtained and optimized. Rheological measurements were conducted in a Rheometrics RAA rheometer with a sample size of 12 mm (dia.)

by 1 mm thickness. The loss moduli (G'') and the elastic moduli (G') were determined at a temperature of 200°C over a frequency range of 0.01 to 1000 rad/s.

Electrical Characterization

Samples were prepared for electrical testing according to the ASTM-257 and ANSI/EOS/ESD-S11.11.1993 specifications. The electrical measurements were taken at two different voltages (100 and 10 volts) to account for high and low resistances, depending on the fiber concentration. For the ASTM measurements, a Keithley 247 high-voltage supply was used to apply the potential to the sample. The sample was inserted in a Keithley 6105, a resistivity adapter with a conveniently dimensioned electrode configuration, which eliminated the need of using silver paint or mercury-filled rings to assure sample contact. This model provides guarded shielded electrodes making sample contact easier, and it accounts for the flatness of the sample. The resultant current was measured with a Keithley 617 programmable electrometer. Four-point probe measurements were made using a point contact four-point probe device and a Kepco power supply. Dielectric strengths were measured using a Hipotronics OC60A with a voltage capacity of up to 60 kV. The sample dimensions were 20 × 15 cm for length and width, respectively. Following the ANSI method, surface and volume resistivities were also measured using a Monroe Model 262A surface resistivity meter and a Monroe Model 268 charge plate analyzer where 47–50% and 25–30% relative humidity (RH) conditions were evaluated. The 47–50% RH tests were performed at room temperature. The 25–30% RH measurements were taken after 48 h soaking in a 25–30% RH environment. Testing was done for the ambient RH environment immediately upon removal from the RH chamber. Charge dissipation measurements were also conducted using the Monroe Model 268. The time required for the voltage to drop across the plates from 5,000 to 500 volts was measured.

RESULTS AND DISCUSSION

Purification and Functionalization

Purifying the VGCFs using a dichloromethane refluxing resulted in highly purified nanofibers.

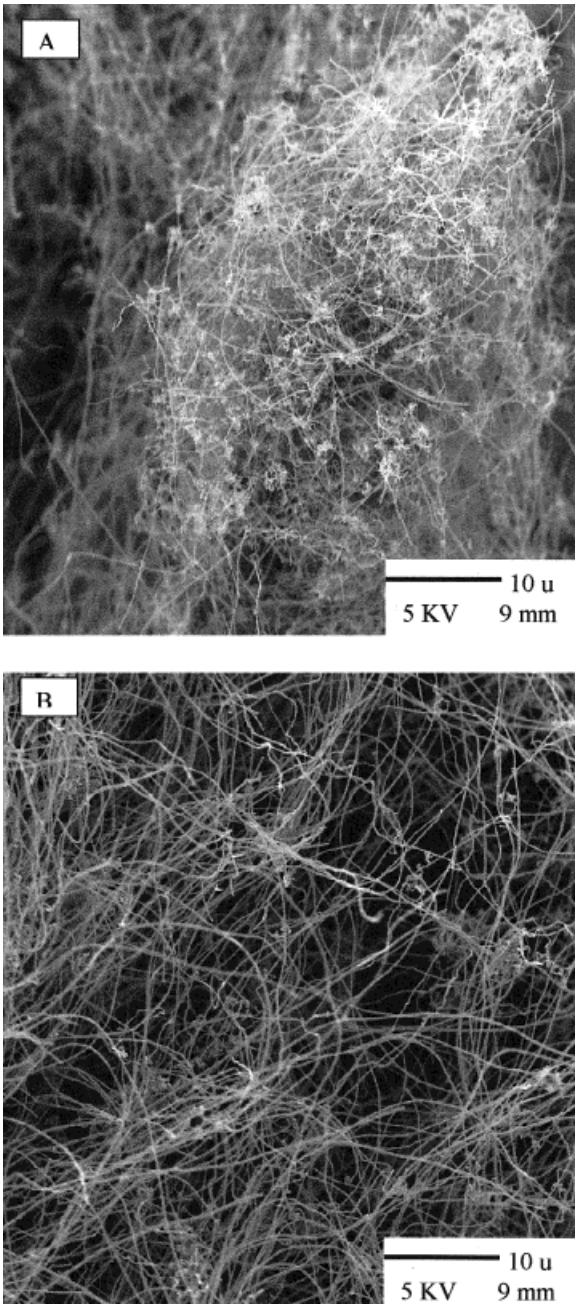

Figure 1 Nanofibers before (A) and after (B) purification procedure.

Figure 1 shows the nanofibers before and after cleaning where the fibers were not shortened and the nanofiber net was made more open. This is significant because an open structure of nanofibers will likely interact more easily with the polymer during mixing; therefore, requiring less shear action to disperse the nanofibers. It was expected that the purification primarily removed the unwanted amorphous carbon and aliphatic

compounds while washing away the metal catalysts. Lozano et al. showed that the CH_2Cl_2 cleaning also attached functional groups on the nanofibers.[37] The various acid washes were also successful at connecting functional groups of —OH, COOH, NO_2, or —CH, although the degree of functionalization and type of functional groups varied with the treatments. Purification with the CH_2Cl_2 and or functionalization with a 2 : 1 mix of nitric and sulfuric acid (65% dilute) produced the higher degree of functional groups over the other oxidation treatments and compared to the as-received condition. The acid functionalization tended to also shorten the nanofibers much like that identified by Friends et al.[44] Functionalization at higher temperatures or for prolonged times tended to reduce the number of functional groups on the nanofibers suggesting that as the defects on the nanofibers are eliminated so are the sites for functionalization. It should also be noted that even though a number of nanofiber conditions were obtained by purification and functionalization, the current article shows results for only the purified nanotubes or for cases where the cleaning processes were not a factor.

Microscopic Analyses

A banbury-type mixer was used to mix the nanotubes in the thermoplastic polymer. Given the size and tendency of agglomeration, this mixing method provides the necessary shear to obtain a uniform distribution of the fibers by exposing the agglomerates to hydrodynamic forces. Evaluation of the degrees of dispersion, absence of polymer degradation, and evaluation of the general rheological data were process optimization indicators. In an ideal dispersion, the fibers should be separated into their smallest unit if structural reinforcement is desirable. Having nanometer-sized fibers, it is likely that the samples will contain agglomerates and networking patterns at high concentrations.[32] Dispersion histograms of micrographs taken at 500× were created and coupled with the standard deviation gave a quantitative description of the dispersion level. The data from the histogram suggest a good level of dispersion. As seen in Figure 2, the histograms for three VGCF concentration levels (2, 9, and 15 wt %) have a normal distribution curve. It can be observed that as the VGCF concentration is increased the histograms drift away form a normal distribution. Lower concentrations were more uniformly dispersed while higher concentrations

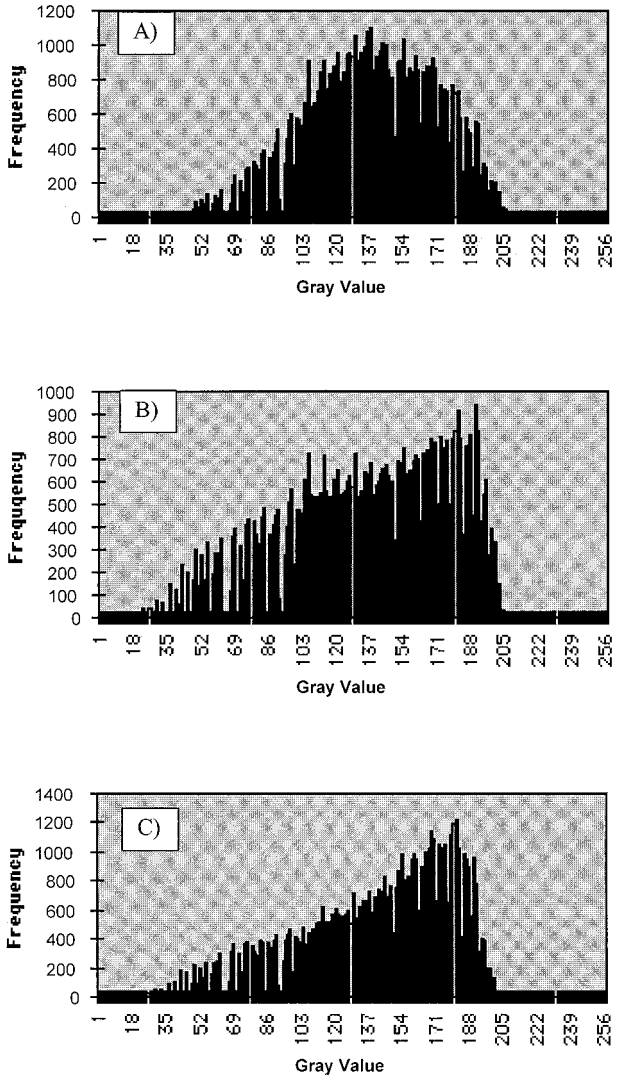

Figure 2 Dispersion histograms of micrographs taken at 365× for (a) 2, (b) 9, and (c) 15 wt % of VGCFs.

tended to disperse and form a network because of more nanofiber self-interactions. It appears that as the concentration of VGCFs increases, there is a composition at which their interaction (touching) tends to alter their distribution toward an interconnected network of sorts, which does not foster continued nanofiber dispersion. Their dispersion is not a segregated network, as previously noted for carbon black and VGCFs. It is, instead, a nanodispersion with perhaps a polymer substructure on the nanoscale. This network can be used as a way to monitor the enhancement of electrical and mechanical properties.

Figure 3 shows a TEM micrograph of fiber distribution in a composite reinforced with 20 wt % of VGCFs where it can be seen that individual

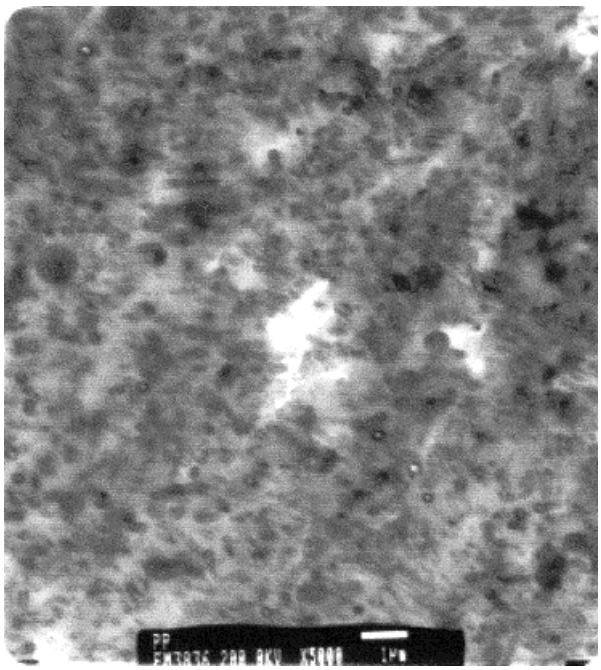

Figure 3 TEM micrograph of a 20% VGCF composite.

separation of the nanofibers as well as an isotropic structure was obtained by the high-shear mixing procedure. Figure 4 shows SEM micrographs where further dispersion of the fibers and their physical interaction with the matrix can be observed. For the optimized samples processed, no indications of porosity were observed. Dispersion and distribution of the VGCFs were achieved where any segregated regions of polymer were likely on the submicron to nanoscale, and of uniform size because of the homogeneous dispersion of the VGCFs.

Rheological Analysis

The torque trace with time for the optimized sample conditions is presented in Figure 5 for pure PP and two different concentrations of VGCFs. Note that there is no change in the degree of steady-state torque. The delay in the start of the onset of torque for the VGCF composites was due to time taken to load in the PP and nanofibers while the mixer was in motion. Mixing parameters of 55–65 rpm increasing to 90 rpm for the last minute were chosen based on process optimization where achieving steady-state mixing with no degradation of the PP was critical for the optimization.

Observation of the effects on melt rheology of increasing the VGCF content shows that the viscosity increases with increasing nanofiber content. Figure 6 shows the typical shear thinning behavior for the complex viscosity observed in PP resins and its composites. Compositions of less than 10 wt % tend to produce a small increase in viscosity and follow closely with the unfilled PP with increasing frequency. Higher VGCF loadings show significant viscosity increases where the observed increase in viscosity can be attributed to

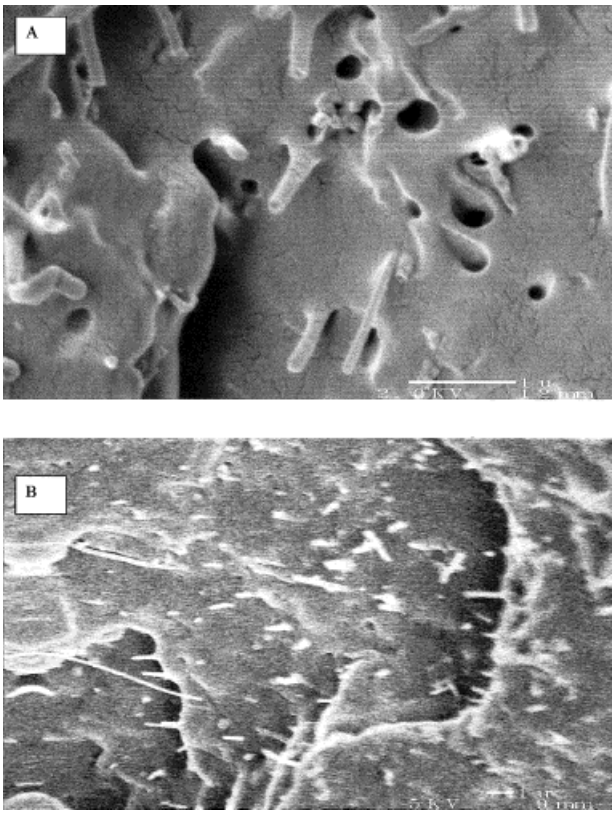

Figure 4 SEM micrograph of (A) 10 wt % and (B) 20 wt % of VGCF composite.

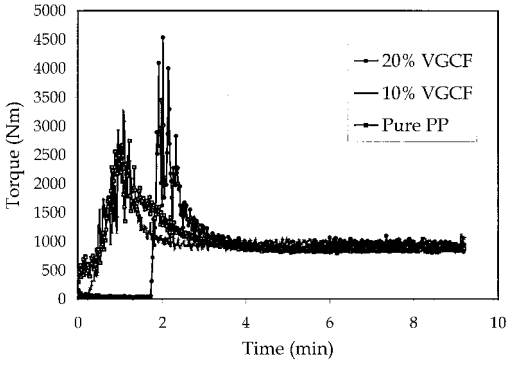

Figure 5 Rheogram for the VGCF reinforced PP composites with different levels of VGCF concentration.

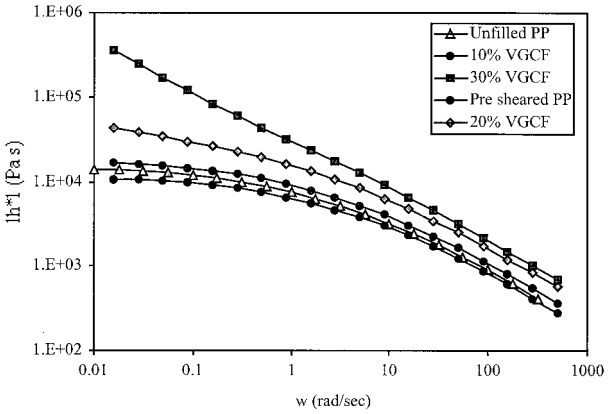

Figure 6 Complex viscosity vs. frequency at 200°C for the VGCF reinforced PP composites at several VGCF concentrations.

fiber wetting (polymer/VGCF interaction). This increase in viscosity at low frequencies with increasing nanofiber content is similar to that seen when processing with MWNTs and SWNTs. Therefore, the significant drop in viscosity at higher frequencies shows that the difficulty of processing with nanotubes is not an issue at higher shear rates. An important aspect to observe from Figure 6 is that the composites become more shear dependent in the low-frequency range as the VGCF concentration is increased. This shear thinning behavior can be attributed to a greater degree of polymer–fiber interaction, which requires higher shear stresses and longer relaxation times for the composite to flow. It is interesting to note that at low shear rates the viscosity seems to exhibit a viscosity threshold at around 10% wt of VGCFs (i.e., the viscosity curve is a tool for identifying the presence of the percolation threshold for this material system).

Viscosity, for cases of filled polymers, can increase very sharply at concentrations just below the maximum packing fraction. The rheological analysis at different processing temperatures reveals that for high flow applications, the samples containing concentrations higher that 20% might be as easy to process as those with low VGCF concentrations, because they show the same viscosity at high shear rates. To observe changes in the viscoelastic parameters, storage (G') and loss (G'') modulus are plotted simultaneously in Figure 7. The frequency at which a crossover point between G' and G'' occurs can be observed. The crossover point shifts to the left and upwards with increasing concentration of VGCF's. At higher VGCF concentrations the elastic modulus increases indicating a higher melt strength. This is a good behavior for applications such as fused deposition modeling (FDM) because the material will keep its shape while it is cooled down. FDM is a rapid prototyping technique where polymer is extruded to form traces of material to make parts by a layer by layer process.

The mixing of the VGCFs with PP showed that the viscosity of the high-temperature melt can be reduced with added shear rate. The rheology also gives us some insight into the nanofiber distribution, and effect on thermophysical properties. Our ability to translate this understanding to systems using nanotubes is at hand because methodologies for producing nanotube-reinforced polymers only requires an order of magnitude increase in the concentration of nanotubes being used. As higher demand on the development of these materials occurs, that transition will easily be made. With nanotubes, entanglements have to be reduced to obtain a high degree of dispersion. It is likely that the shear mixing of the banbury mixer will lead to this high dispersion. Removing the nanotubes from the ropes may have to occur by other means.

Electrical Properties

Surface resistivity vs. VGCF wt % concentration is shown in Figure 8. Data points for PP and PE mixed with different wt % of VGCFs, and a 5 wt % of as-received SWNTs mixed with a Shell Epon epoxy are plotted in Figure 8. The charge dissipation times were found to be of 0.1 s for all the samples with concentration higher than 10 wt %. Below this concentration the samples could not dissipate effectively. The epoxy/SWNT data point

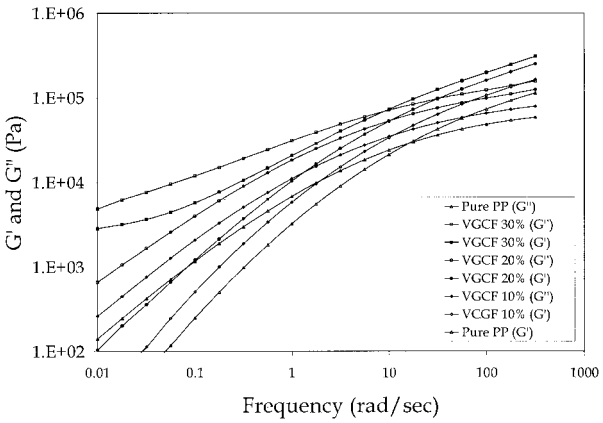

Figure 7 Storage and loss modulus vs. frequency at 200°C of VGCF reinforced PP composites.

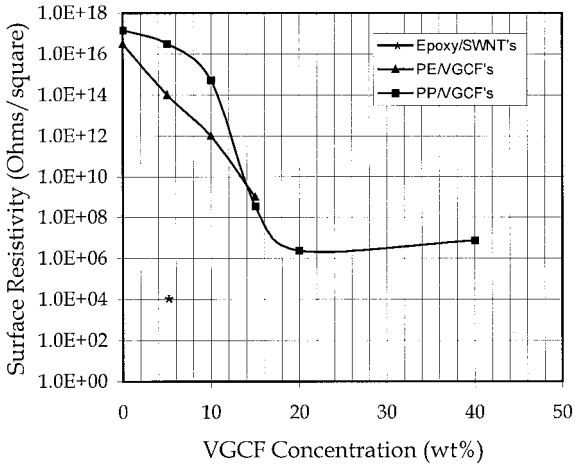

Figure 8 Surface resistivity values vs. VGCF concentration.

suggests that SWNTs will likely lead to lower percolation values, and may lead to EMI materials. The samples tested showed stability at different relative humidity RH conditions, demonstrating their capability to be used over a broad range of atmospheric conditions. From Figure 9 it can be observed that the volume resistivity of PP/VGCF samples follows the same trend as the surface resistivity with a similar percolation threshold. For both measurements, the resistivity on the VGCF composites dropped around 10 orders of magnitude when the VGCF reached a critical concentration. The measurements, performed at 100 and 10 volts, produced no significant difference.

The critical point at which the VGCF-reinforced polypropylene composites become dissipative is between 9 and 18 wt % of VGCFs. As it has been studied, volume resistivity is not only dependent on filler concentration but also on filler distribution and particle morphology. The aspect ratio of the fillers plays an important role on the concentration of reinforcement necessary to achieve percolation.[1] The percolation theory predicts that the larger the aspect ratio, the smaller the volume fraction required to achieved percolation. Work conducted by Lozano with Cu powders ($l/d \approx 1$) showed that a concentration of 15% was required to start the percolation threshold.[19] Dutta et al.[12] worked with Al particles in which a concentration close to 35% was required. Carbon black-filled materials can require loadings exceeding 20 wt % and as high as 40 wt %. Such high concentrations compromise the physical properties of the matrix. Cases where low amounts of nanofibers (<1 wt %) are used in a segregated network also compromise the mechanical properties, and do not lead to multifunctional materials.

Electrical measurements were also conducted by a four-point probe method to study the voltage sensitivity of the composite, and the resistivity trace is shown in Figure 10 as a function of VGCF concentration. A nonohmic (nonlinear dependence of current on voltage) behavior within the observed percolation threshold range was observed. This type of behavior is therefore considered as evidence of the tunneling process of electrons in the percolation range (9–18%) observed by the ASTM and ANSI measurements. Increasing the VGCF concentration therefore surpasses the percolation threshold range, and an ohmic behavior is achieved. The conduction mechanism after the percolation threshold (above 18%) can be described as the passage of electrons in a network of fibers with intimate contact where there is no need to surpass any internal resistance. Given

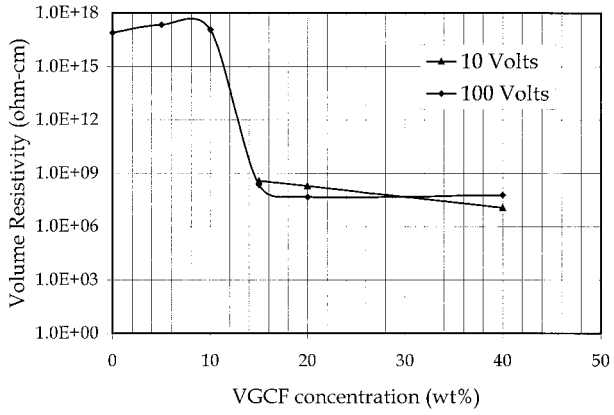

Figure 9 Volume resistivity values vs. VGCF concentration.

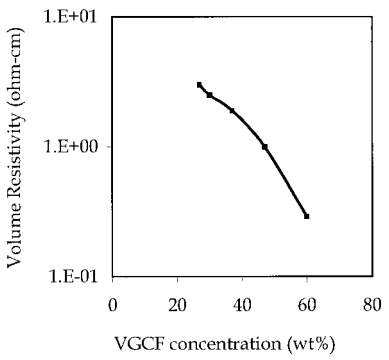

Figure 10 Volume resistivity vs. VGCF concentration studied by the four-point probe method.

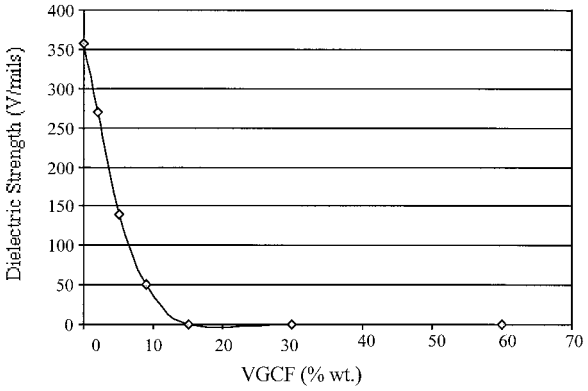

Figure 11 Dielectric strength of VGCF-reinforced PP composites.

this, further increase in loading was not expected to cause any significant decrease in resistivity. Figure 11 shows the dielectric breakdown characteristics of the various PP/VGCF sheet samples. Note that the voltage drops to a significantly small level of resistance as the concentration of VGCF reaches the segregated network.

The results obtained from volume and surface resistivity measurements lead to the conclusion that a new ESD material has been developed. The VGCF-reinforced PP composites, along with the conducting polymers using the other polymers in this study, are highly dispersed nanofibers in thermoplastic polymers that have the potential of being multifunctional materials for strength and electrical conduction. The dissipation times show that the charge generated is quickly removed from the polymer, which was highly insulating prior to nanofiber mixing.

CONCLUSION

A homogeneous state of nanofibers dispersed in thermoplastic polymers has been obtained where these nanofibers contribute to the electrostatic dissipation properties of advanced composites. An absence of porosity with reliable wetting and a static dissipative composite has been achieved. An understanding of the processing conditions has been established based on rheological parameters. It is observed that by going to high shear rates the process viscosity is reduced and mixing is easily accommodated, which produces a high degree of nanofiber dispersion. This knowledge will promote the development of SWNTs and other type of nanofiber-reinforced thermoplastic systems.

The authors would like to acknowledge the support received from National Science Foundation under grant number DMR-9357505, the Texas Higher Education Board under grant number 003604-056, the National Aeronautics and Space Administration under grant number NCC 9-77, and the Consejo Nacional de Ciencia y Tecnologia (CONACYT), which led to the completion of this work. The authors would also like to acknowledge the help of Shana Diez and Catherine Arthur, the Receiving Testing and Inspection Facility at the NASA Johnson Space Center, Houston, TX, and the use of facilities at Conductores Monterrey, Monterrey, Mexico, toward the completion of this work.

REFERENCES

1. Bhattacharya, S. K. Metal-Filled Polymers; Marcel Dekker, Inc.: New York, 1986.
2. Seanor, D. A. Electrical properties of Polymers; Academic Press, Inc.: New York, 1982.
3. Blythe, A. R. Electrical Properties of Polymers; Cambridge University Press: Cambridge, UK, 1979.
4. Margolis, J. M. Conductive Polymers and Plastics; Chapman and Hall, Ltd.: London, UK, 1989.
5. Breuer, O.; Tchoudakov, R.; Narkis, M.; Siegmann, A. J Appl Polym Sci 1999, 73, 1655.
6. Charbonneau, R. 43rd Int SAMPE Symp 1998, 833.
7. Wienhold, P. D.; Mehoke, D. S.; Roberts, J. C.; Seylar, G. R.; Kirkbride, D. L. 30th Int SAMPE Tech Conf 1998, 243.
8. Yi, X. S.; Wu, G.; Pan, Y. Polym Int 1997, 44, 117.
9. Franey, J. P.; Freund, R. S. Mater Res Soc Symp Proc 1992, 265, 267.
10. U.S.A. Pat. #4.590.623 Kitchman, F. E. (1986).
11. U.S.A. Pat. #5.820.788 Smith, W. N. (1998).
12. Dutta, A. L.; Singh, R. P. J Vinyl Technol 1992, 14.
13. Petrovic, Z. S.; Martinovic, B.; Divjakovic, V.; Budinski-Simendic, J. J Appl Polym Sci 1993, 49, 1659.
14. Miyasaka, K.; Watanabe, K.; Jojima, E.; Aida, H.; Sumita, M.; Ishikawa, K. J Mater Sci 1982, 17, 1610.
15. Ghofraniha, M.; Salovey, R. Polym Eng Sci 1988, 28, 58.
16. Bhattachayra, S.; Basu, S.; De, S. K. J Appl Polym Sci 1980, 25, 111.
17. Tchoudakov, R.; Breuer, O.; Narkis, M.; Siegmann, A. Polym Eng Sci 1996, 36, 1336.
18. U.S.A. Pat. #5.744.573 Brubaker, L. C. (1998).
19. Garza, R.; Lozano, K.; Guerrero, C. Mmeorias de Compositos 1993; Saltillo, Coahuila: Mexico, 1993.
20. Mather, P. J.; Thomas, K. M. J Mater Sci 1997, 32, 401.

21. Mather, P. J.; Thomas, K. M. J Mater Sci 1997, 32, 1711.
22. Bow, K. E. IEEE Transact Power Deliv 1990, 5.
23. Sandler, J.; Shaffer, M. S. P.; Prasse, T.; Bauhofer, W.; Schulte, K.; Windle, A. H. Polymer 1999, 40, 5967.
24. Alig, R. L. Tech Data Sheet Appl Sci 1996, May.
25. Anderson, D. P.; Ting, J. M.; Lake, M. L.; Alig, R. L. 22nd Biennal Conference on Carbon; American Chemical Society: San Diego, CA, July 16–21, 1995.
26. Alig, R. L.; Ting, J. The European Carbon Conference "Carbon 96"; Newcastle, UK, July 1996.
27. Jin, L.; Bower, C.; Zhou, O. Appl Phys Lett 1998, 73, 1197.
28. Zhong, T.; Xu, H. Macromolecules 1999, 32, 2569.
29. Lozano, K.; Zheng, A.; Mayeaux, B.; Espinoza, N.; Yowell, L.; Provenzano, V.; Shull, R.; Files, B.; Bonilla-Rios, J.; Barrera, E. V. Proceedings of a Symposium sponsored by The Powder Materials Committee from The Minerals, Metals and Materials Society (TMS), 1999, p. 341.
30. Caldeira, G.; Maia, J. M.; Carneiro, O. S.; Covas, J. A.; Bernardo, C. A. ANTEC 1997, 403.
31. Ting, J. M.; Lake, M. L.; Duffy, D. R. J Mater Res 1995, 10, 1478.
32. Hess, W. M.; Swor, R. A.; Micek, E. J. Rubber Chem Technol 1983, 57, 959.
33. Bani-Hani, M.; Banu, D.; Campanelli, J.; Feldman, D. J Appl Polym Sci 1999, 74, 1156.
34. Palit, K. ANTEC 85, 1985, 506.
35. Chazeau, L.; Cavaille, J. Y.; Canova, G.; Dendievel, R.; Boutherin, B. J Appl Polym Sci 1999, 71, 1797.
36. Tjong, S. C.; Meng, Y. Z. J Appl Polym Sci 1999, 72, 501.
37. Lozano, K.; Files, B.; Rodriguez-Macias, F. J.; Barrera, E. V. Proceedings of a Symposium sponsored by The Powder Materials Committee from The Minerals, Metals and Materials Society (TMS), 1999, p. 333.
38. http://www.apsci.com/asi.
39. http://www.fibrils.com.
40. Lozano, K.; Barrera, E. V. J Appl Polym Sci, to be published.
41. Files, B. S.; Mayeaux, B. M. Adv Mater Process 1999, 156, 47.
42. Ajayan, P. M.; Redlick, P.; Rühle, M. J Microsc 1997, 185, 275.
43. Shekhar, S. Adv Mater 1998, 10, 1157.
44. U.S.A. Pat. #5.611.964 Friend, S. O.; Barber, J. J. (1997).
45. Selliti, C.; Koening, J. L.; Ishida, H. Carbon 1990, 28, 221.